Journal of Hydroscience and Hydraulic Engineering
Vol. 17, No.2 November, 1999, 97-105

ANALYSIS OF BED TOPOGRAPHY IN A COMPOUND MEANDERING CHANNEL USING A 3-D NUMERICAL MODEL WITH ASSUMPTION OF HYDROSTATIC PRESSURE

By

Shoji FUKUOKA

Ph.D., D.Eng, Professor, Faculty of Engineering, Hiroshima University (1-4-1, kagamiyama, Higashi-hiroshima, 739-8527 Japan).

Akihide WATANABE

D.Eng. Associate professor, Faculty of Engineering, Hiroshima University (ditto).

And

Shoji OKADA

Graduate Student, Hiroshima University (ditto).

SYNOPSIS

For the evaluation of flow structures and river bed forms in a compound meandering channel, a three dimensional numerical model was used. This model uses the boundary fitted curvilinear system (ξ,η,σ) and the spectral method to calculate the flow velocity distribution, water surface and bed variations. In this paper, applicability of this model was examined by comparison with laboratory experiments on bed deformation for this sort of channels. According to the results obtained from the application of the hydrostatic pressure model, scour occurred only at the outer bank of the bends where the flow was concentrating. However, in the laboratory experiments this kind of scouring did not happen for flows with high relative depth values. Therefore, it was considered that the use of a hydrodynamic pressure model is necessary for evaluating the deformation in a compound meandering channel with high relative depth values.

Key Words: meandering compound channel, river bed deformation, 3D analysis of flows, spectral method, hydrostatic pressure

1. INTRODUCTION

Previous researchers (1,2,3,4,5) showed that flow field and bed profile in a compound meandering channel differ greatly from those of bankful flows for floods in which the depth over the flood-plain has a considerable magnitude respect to the bankful-depth in the main channel. Among these differences first, the maximum velocity filament in the main channel runs near the inner banks; regarding the secondary flows, the rotation is reversed from that observed in bankful flows (6,7,8). These changes in the flow fields are accompanied by the cessation of scouring at outer bank bed and by the scouring near the inner bank (6,9).

It is generally believed that these flow characteristics are depending on the sinuosity and the phase difference between the main channel alignment and levee alignment, relative depth, ratio of roughness and width between flood channel and main channel, and so on. The effects of relative depth and sinuosity were shown by large-scale hydraulic experiments performed by Fukuoka *et al.* (9), and by the flow velocity distributions calculated from actual aerial surveying photographs (10).

It has been shown that the geometrical and hydraulic conditions affect

dramatically the features of the flow structure in a compound meandering channel, therefore numerical analysis should be used to compute flow variables and bed evolution. Therefore, efforts are made to develop three-dimensional numerical models that might represent compound meandering flows. Jin and Egashira *et al.* (11) developed a two-layer model and then a three-dimensional statistical turbulence model which is applicable for the flows of low relative depth.

The authors developed a numerical model that uses the spectral method to express three-dimensional flows in compound meandering channels with fixed bed (14,15) and capable to express the changes in the structure of flow due to the changes in the relative depth (15). However, to the authors knowledge no model has been developed to reproduce bed profiles accurately in compound meandering channels.

This paper describes the experimental analysis performed by incorporating bed variations into a 3-D flow model (14,15) developed by the authors, and discusses its suitability and limitation. Due to the considerable large computation time of bed variation, the authors used a simplified numerical model that assumes hydrostatic pressure.

2. METHOD OF ANALYSIS

1) Introduction of the plane curve coordinate system and σ coordinate system

Coordinate transformation is used as a simple way to incorporate the effects of the complex boundary profile into the numerical analysis. Fig. 1 shows the plane profile of the compound channel to be analyzed, together with the coordinate system. The plane coordinate systems are transformed from rectangular ones (x,y) to curvilinear ones (ξ,η). As shown in Fig. 2, the vertical coordinate system z is transformed into σ coordinate system, which is defined as

$$\begin{cases} z = z_p + (z_o - z_p)\sigma, & (\sigma \geq 0) \\ z = z_p + (z_p - z_b)\sigma, & (\sigma < 0) \end{cases} \tag{1}$$

where z_o, z_p and z_b represent water surface, flood channel and bed heights respectively. The values σ = 1, 0, -1 represent the references for surface, flood channel and bed heights, respectively. At this time, the scale parameters relating to the vertical axis are respectively represented by using depths above and below a flood channel:

$$\begin{cases} z_\sigma = (z_o - z_p), & (\sigma \geq 0) \\ z_\sigma = (z_p - z_b), & (\sigma < 0) \end{cases} \tag{2a}$$

$$z_\xi = \frac{\partial z_p}{\partial \xi} + \{\frac{\partial}{\partial \xi}(z_\sigma)\}\sigma \tag{2b}$$

$$z_\eta = \frac{\partial z_p}{\partial \eta} + \{\frac{\partial}{\partial \eta}(z_\sigma)\}\sigma \tag{2c}$$

If z_o and z_p are constant, the metric tensors can be evaluated from changes in the bed surface or the depth below the flood channel alone, without having to incorporate mesh movement. Thus, a coordinate system results in the following metric tensor matrix:

$$\begin{bmatrix} T_t & \xi_t & \eta_t & \sigma_t \\ T_x & \xi_x & \eta_x & \sigma_x \\ T_y & \xi_y & \eta_y & \sigma_y \\ T_z & \xi_z & \eta_z & \sigma_z \end{bmatrix} = \begin{bmatrix} 1 & 0 & 0 & -z_t / z_\sigma \\ 0 & y_\eta / J' & -y_\xi / J' & -(z_\xi \xi_x + z_\eta \eta_x)/z_\sigma \\ 0 & -x_\eta / J' & x_\xi / J' & -(z_\xi \xi_y + z_\eta \eta_y)/z_\sigma \\ 0 & 0 & 0 & 1/z_\sigma \end{bmatrix} \tag{3a}$$

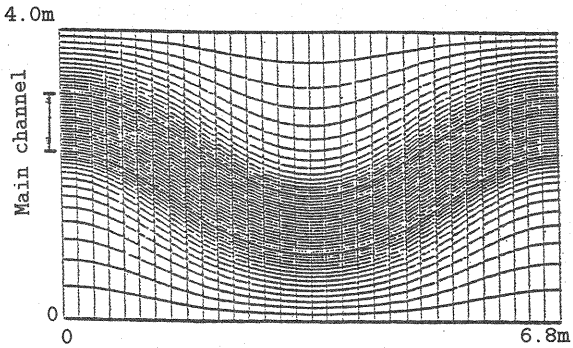

Fig. 1 Compound channel plane profile and plane coordinate system

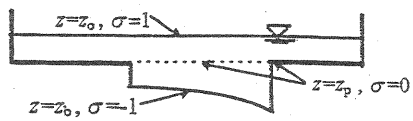

Fig.2 Definition of σ coordinate system

$$J = J' z_\sigma, \quad J' = x_\xi y_\eta - x_\eta y_\xi \tag{3b}$$

where subscripts in the coordinate system indicate the partial differentiation of that coordinate, t represents time, and J the Jacobian. Contravariant flow velocity is represented in the curvilinear coordinate system as follows:

$$\begin{cases} U = \xi_x u + \xi_y v \\ V = \eta_x u + \eta_y v \\ W = \sigma_z W' = \sigma_z (\sigma_x' u + \sigma_y' v + w) \end{cases} \tag{4}$$

where $u = x$-direction flow velocity; $v = y$-direction flow velocity; $w = z$-direction flow velocity; $U = \xi$-direction contravariant flow velocity; $V = \eta$-direction contravariant flow velocity and $W = \sigma$-direction contravariant flow velocity. In equation (4), σ_x' and σ_y' represent the quantities defined by $\sigma_x = \sigma_x' \sigma_z$, $\sigma_y = \sigma_y' \sigma_z$.

2) Basic equations of the flow

When the coordinate system is introduced as described above, the equation of motion that approximates the hydrostatic pressure is expressed as follows:

$$\frac{\partial u}{\partial t} + U\frac{\partial u}{\partial \xi} + V\frac{\partial u}{\partial \eta} + (W' + \sigma_t')\frac{\partial u}{\partial z'} = g_x - \frac{1}{\rho}\left(\xi_x \frac{\partial \zeta}{\partial \xi} + \eta_x \frac{\partial \zeta}{\partial \eta}\right) + \nu_T \Delta u \tag{5a}$$

$$\frac{\partial v}{\partial t} + U\frac{\partial v}{\partial \xi} + V\frac{\partial v}{\partial \eta} + (W' + \sigma_t')\frac{\partial v}{\partial z'} = g_y - \frac{1}{\rho}\left(\xi_y \frac{\partial \zeta}{\partial \xi} + \eta_y \frac{\partial \zeta}{\partial \eta}\right) + \nu_T \Delta v \tag{5b}$$

where g_x, g_y = gravitational acceleration in the respective directions; and ζ = water level fluctuation relative to the reference surface. The eddy viscosity ν_T is expressed in the following equation using h = depth from the reference surface, z_d = height from the bottom, and u_* = bottom friction velocity.

$$\nu_T = \kappa u_* z_d (1 - z_d / h) \tag{6}$$

where

$$\Delta = \alpha \frac{\partial^2}{\partial \xi^2} + 2\beta \frac{\partial^2}{\partial \xi \partial \eta} + \gamma \frac{\partial^2}{\partial \eta^2} + (\nabla_H^2 \xi)(\frac{\partial}{\partial \xi} - z_\xi \frac{\partial}{\partial z'}) + (\nabla_H^2 \eta)(\frac{\partial}{\partial \eta} - z_\eta \frac{\partial}{\partial z'})$$
$$- 2(z_\xi \alpha + z_\eta \beta) \frac{\partial}{\partial \xi}(\frac{\partial}{\partial z'}) - 2(z_\xi \beta + z_\eta \gamma) \frac{\partial}{\partial \eta}(\frac{\partial}{\partial z'}) - (\alpha z_{\xi\xi} + 2\beta z_{\xi\eta} + \gamma z_{\eta\eta}) \frac{\partial}{\partial z'}$$
$$+ (1 + \alpha z_\xi^2 + 2\beta z_\xi z_\eta + \gamma z_\eta^2) \frac{\partial}{\partial z'}(\frac{\partial}{\partial z'}) \; ;$$

$$\frac{\partial}{\partial z'} = \frac{1}{z_\sigma}(\frac{\partial}{\partial \sigma}); \quad \nabla_H^2 = \frac{\partial^2}{\partial x^2} + \frac{\partial^2}{\partial y^2}; \quad \alpha = (\xi_x^2 + \xi_y^2); \; \beta = (\xi_x \eta_x + \xi_y \eta_y); \; \gamma = (\eta_x^2 + \eta_y^2)$$

The continuity equation is expressed as

$$\frac{\partial J' z_\sigma U}{\partial \xi} + \frac{\partial J' z_\sigma V}{\partial \eta} + \frac{\partial J' W'}{\partial \sigma} = 0 \tag{7}$$

Integration of Eq. (7) from the bed surface (σ=-1) to the water surface ($z = z_o + \zeta$) produces Eq. (8), and ζ indicates water level fluctuation:

$$J(\frac{\partial \zeta}{\partial t} - \frac{\partial z_b}{\partial t}) + \frac{\partial}{\partial \xi}\int_{-1}^{\sigma(z_o+\zeta)} J' z_\sigma U d\sigma + \frac{\partial}{\partial \eta}\int_{-1}^{\sigma(z_o+\zeta)} J' z_\sigma V d\sigma = 0 \tag{8}$$

The kinematic boundary conditions are used to assign the σ-direction contravariant flow velocity W' at the water surface and bed surface, and they are expressed by Eq. (9):

$$\begin{cases} \dfrac{\partial \zeta}{\partial t} + U \dfrac{\partial \zeta}{\partial \xi} + V \dfrac{\partial \zeta}{\partial \eta} = W', (z = z_o + \zeta) \\ \dfrac{\partial z_b}{\partial t} = W', \qquad (\sigma = -1) \end{cases} \tag{9}$$

3)Basic equations of the bed deformation

Quantitative bed variation is determined by using the sediment continuity equation as follows:

$$J' \frac{\partial z_b}{\partial t} + \frac{1}{1-\lambda}(\frac{\partial J' q_{B\xi}}{\partial \xi} + \frac{\partial J' q_{B\eta}}{\partial \eta}) = 0 \tag{10}$$

where, $(q_{B\xi}, q_{B\eta})$ is the contravariant sediment discharge vector for the coordinate systems (ξ, η).

$$\begin{cases} q_{B\xi} = q_B \{\dfrac{U_b}{\sqrt{u_b^2 + v_b^2}} - \dfrac{1}{\sqrt{\mu_s \mu_k}} \dfrac{u_{*c}}{u_*}(\alpha \dfrac{\partial z_b}{\partial \xi} + \beta \dfrac{\partial z_b}{\partial \eta})\} \\ q_{B\eta} = q_B \{\dfrac{V_b}{\sqrt{u_b^2 + v_b^2}} - \dfrac{1}{\sqrt{\mu_s \mu_k}} \dfrac{u_{*c}}{u_*}(\beta \dfrac{\partial z_b}{\partial \xi} + \gamma \dfrac{\partial z_b}{\partial \eta})\} \end{cases} \tag{11}$$

This is obtained through the coordinate transformation of the longitudinal and transverse sediment discharge vector (16) that incorporates the effects of the bed gradient. Here, q_B= bed load, μ_s= static friction factor, μ_k= dynamic friction factor, u_{*c}= critical friction velocity, and the subscript b indicates the value at

the bed. This analysis employs the Ashida-Michiue equation for sediment discharge, which is calculated to incorporate additional tractive force and changes in critical tractive force (17) due to the bed slope change.

4) Introduction of spectral method and formulation.

Because the profile of the boundary and the flow field change periodically in the longitudinal direction, Fourier series expansions are applied for the plane boundary profile, the flow field and the bed profile in this direction. The spectral collocation method is employed to solve the differential equation. For this analysis, the series is expanded from the 0th mode to the 7th mode, and 32 spectral collocation points were selected.

For the flow field analysis, a longitudinal differentiation was calculated by differentiating in the spectral space and then inverting the value to the spectral collocation point through inverse Fourier transformation. Regarding to the differentiation of the connective terms in (η,z) plane, an upwind difference of the 3rd order in the transverse direction and of 1st order in the vertical direction are used.

5) Boundary conditions and their method of calculation

Using the procedure outlined in section 4), velocities u, v and water level ζ are calculated on the spectral points and then time-integrated in spectral space. The time integrals of velocity and water level are explicitly calculated with the Huen method, which is 2nd order accuracy in time. The vertical component of the flow is determined using the continuity equation.

The bed deformation is very slow in comparison with the velocity adjustment, therefore, the time variations of bed and velocity are repeatedly calculated at separate time scales in this analysis. Time distortion in bed variation relative to the flow was limited to between 6 and 12.

The resistance at the walls which was taken proportional to the square of the velocity in the vicinity, being assigned as a boundary condition for velocity. Also impermeable slip-conditions are applied at the walls. Friction velocities on side walls and the bottom are determined by dividing velocities near the walls and the bed by the resistance coefficient, respectively.

3. BED DEFORMATION ANALYSIS

1) Conditions for experimentation and calculation

The plane profile of the compound channel is shown in Fig. 1, where the total width = 4.0 m; main channel width = 0.8 m; mean main channel bank height = 0.055 m; meander length = 6.8 m; and sinuosity = 1.1. There are five and two vertical points below and above the flood channel height, respectively.

The authors analyzed Cases 2 and 3 in the large-scale experiment performed by Fukuoka *et al* (9). The experimental channel made of concrete was 15 m in total length. The flood channel was covered with artificial turf to create the appropriate roughness and the main channel was filled with sand 0.8 mm in diameter. The slope of the channel and bed was 1/600. The resistance coefficient at the bottom was calculated by using the equivalent roughness k_s and $z_{1/2}$ as

$$\varphi_b = 5.75\log(z_{1/2} / k_s) + 8.5 \qquad (12)$$

where $z_{1/2}$ is the height in the center of the 1st bottom mesh which is the calculation point for flow velocity. It was assumed that k_s= 2.8 cm in the flood channel. Because of the low tractive force, a value of 110% of the sand diameter was used for the value of k_s at the bottom, but it did not include the resistance due to sand wave.

Table 1 Conditions for analysis

Case	Discharge (*l*/s)	Main channel depth (cm)	Flood channel depth (cm)	Relative depth Dr
2	24.9	7.4	1.9	0.26
3	35.9	8.0	2.5	0.31

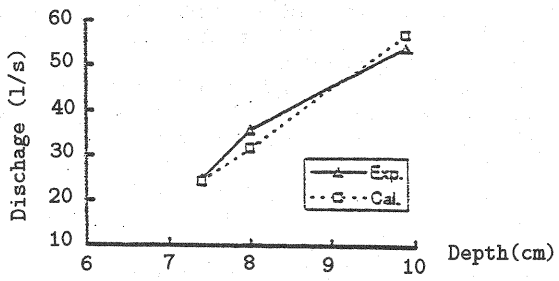

Fig. 3 A comparison of observed and calculated discharge

Table 1 gives the conditions of numerical analysis. For this analysis, the conditions were decided to produce a depth (i.e., relative depth) equivalent to that used in the experiment, and the resistance coefficient was fixed so that the calculated discharge would match the experimental discharge. Fig. 3 gives the calculated discharges of flat-bed and the discharges after bed deformation in the experiments. The comparison between these values and the experimentally observed results shows that the method of assigning the resistance coefficient is reasonable.

2) Bed variations

Figs. 4 and 5 show the observed and calculated bed variations respectively in the main channel for Case 2, where both figures display the bed profiles by contour lines after 3 and 5 hours of flow. Figs. 6 and 7 show similar results for Case 3. In both the cases the flow proceeds from the right to left. The experimental results show bed variation of one wave length in the central part of the meandering channel.

Figs. 4 and 5 indicate poor agreement in shape. In the experimental results, bed scouring occurs from the channel center in the maximum curvature point and extending towards the inflection point of the outer bank, but the calculation shows a scouring region spreads out from the outer bank to the inner bank and the maximum scouring occurs at the inner bank in the point of maximum curvature. The calculated bed variation has not yet achieved a steady state, with a scouring region moving downstream gradually. On the other hand, the calculations depict accurately both position and shape of deposition above 2 cm.

Comparing Fig. 6 with Fig. 7, we find that the calculated scouring region is located near the inner bank at the maximum curvature region and the outer bank's inflection point while the observed results indicate bed scouring extending from the center to the inner bank at the maximum curvature region. The calculations also suggest a larger deposition range and height than the observed results. On the contrary, as shown in Figs. 5 and 6, the bed profile calculated with the conditions of Case 2 resembles more closely the observed profile in Case 3, with a scouring region that apparently would come to resemble the observed scouring region as it moves downstream.

Fig. 7 shows the inner bank scouring at the maximum curvature and coincided with the experiments. Fig. 6 indicates no such scouring at the inflection point. In the mathematical model, this scouring results from the concentration of the flow below the flood channel height near the outer bank. A comparison of Figs. 5 and 7

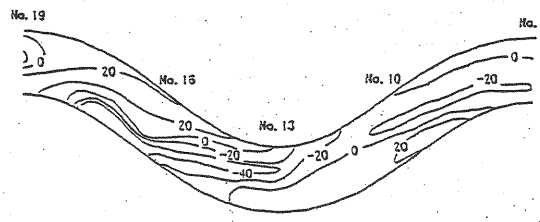

a) After 3 hours (unit = mm)

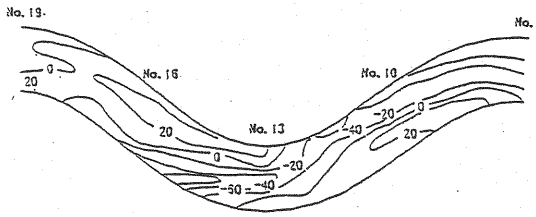

b) After 5 hours (unit = mm)

Fig. 4 Bed variation contour in Case 2 (observed results)

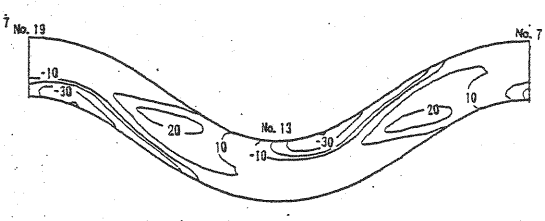

a) After 3 hours (unit = mm)

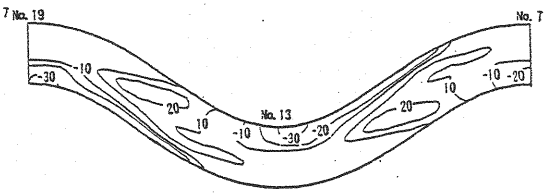

b) After 5 hours (unit = mm)

Fig. 5 Bed variation contour in Case 2 (calculation results)

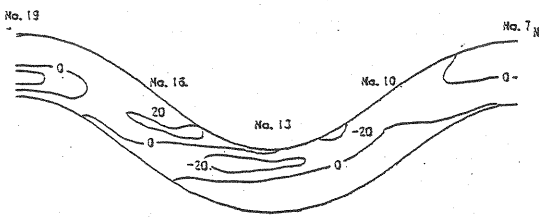

a) After 3 hours (unit = mm)

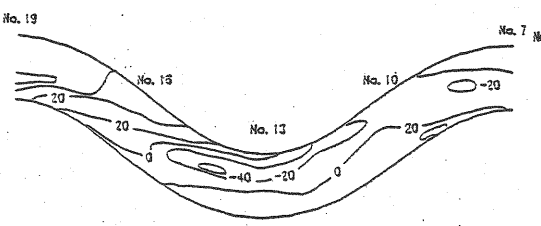

b) After 5 hours (unit = mm)

Fig. 6 Bed variation contour in Case 3 (observed results)

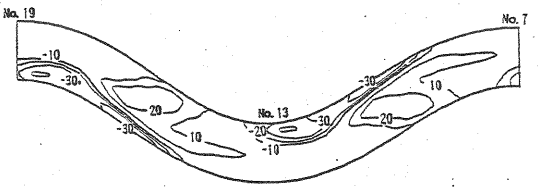

a) After 3 hours (unit = mm)

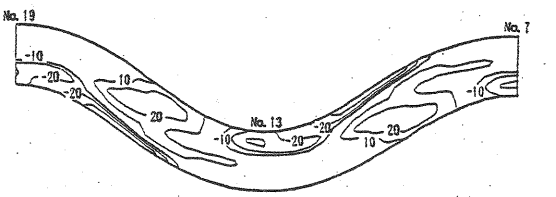

b) After 5 hours (unit = mm)

Fig. 7 Bed variation contour in Case 3 (calculation results)

shows that this tendency is stronger at large relative depths. Although it is not described in this paper, larger relative depths would further increase the flow's concentration, resulting in considerable scouring and precluding the expression of a realistic bed variation.

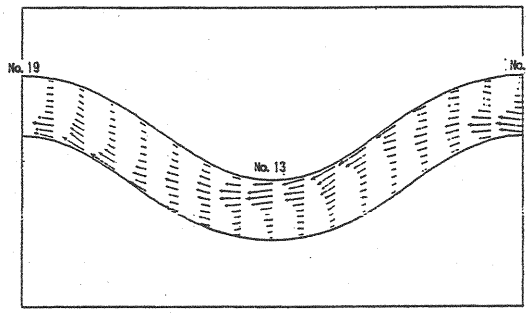

Fig. 8 Calculated vector of depth-averaged velocity below flood channel height in Case 3 (after 5 hours)

Fig. 8 shows the depth-averaged velocity vectors below the flood channel height for Case 3 (after 5 hours of flow). This indicates that the flow is concentrated and accelerated considerably near the outer bank at the inflection point as it moves toward the inner bank. The flow concentration at this point causes an extensive scouring and a wider region of deposition on the opposite bank and a larger scouring depth causes the flow to concentrate even more. Such a bed variation could not be observed in the results of experiments, therefore flows in actual rivers do not concentrate to this degree. This concentration of the flow indicated by the calculations is most likely a result of the approximation of hydrostatic pressure. This area of flow concentration is where the assumption of hydrostatic pressure does not hold well. In the case of a fixed bed, the differences between results obtained with assumption of the hydrostatic pressure and results obtained without such assumption are small, but in the outer bank at the inflection point, the degree of flow concentration with the assumption of the hydrostatic pressure is different from one without such assumption (14). It may be surmised that the assumption of hydrostatic pressure prevents the accurate representation of flow fields in the calculations although the flow concentration would be weakened due to a rise in pressure. Therefore, for a reduction in the flow concentration, it is necessary to calculate the flow field without assuming hydrostatic pressure.

The difference between observed and calculated results for the position and size of maximum scouring in bed deformation are due to the use of periodic boundary conditions in the calculations and the effects of sand waves in the experimentation in which the bed variation was not actually periodic. Effects of the development and progress of these sand waves resulted in bed variation for each case, so the position and size of maximum scouring differed slightly from the calculated values.

4. Conclusions

The following was obtained by an analysis of bed deformation in compound meandering channels with flow assessment based on a three-dimensional numerical model which has an assumption of hydrostatic pressure. The scouring near the inner bank of the main channel and the downstream deposition of the inner bank observed in the experiments were also indicated by the results of this analysis. However, the analysis also suggests that the flow concentrates at the outer bank near the inflection point of the main channel, indicating scouring which is not observed experimentally. The cause of this discrepancy is believed to be the assumption of hydrostatic pressure in that area, albeit a narrow one, where hydrostatic pressure does not actually occur.

For this reason it is necessary to analyze bed deformation using a method that does not assume hydrostatic pressure and to compare the results of the method with those of experimentation and to verify the validity of three-dimensional numerical models used to analyze bed deformation in compound meandering channels.

References

1. Ashida, K., S. Egashira, B. Liu and M. Takiguchi : Flow characteristics and bed variations in a meandering channel with flood plains, Annuals Disaster Prevention Research Institute, Kyoto University, No.32B-2, pp.527-551, 1989, (in Japanese).
2. Kinoshita, R. : Experimental study concerning field work of alluvial phenomena at flooding and best possible river course example, Control of Flood Flows in Fluvial Rivers and Improvement of Safety of River Channel during Flood, Report of Scientific Research Fund, No.A-62-1, pp.63-168, 1988, (in Japanese).
3. Mori, A. : Three dimensional analysis of meandering open channel flow, Control of Flood Flows in Fluvial Rivers and Improvement of Safety of River Channel during Flood, Report of Scientific Research Fund, Ministry of Education, No.A62-1, pp.91-104, 1986, (in Japanese).
4. Mori, A. and T. Kishi : The characteristics of river bed topography of Ishikari-river observed on the Flood in 1981, Proc. of the 30th Japanese Conference on Hydraulics, pp.493-498, 1986, (in Japanese).
5. Ashida, K., S. Egashira, and B. Liu : A study of the hydraulics of meandering compound channel flows, Proceedings of the Hydraulic Engineering, JSCE, Vol.34, pp.397-402, 1990, (in Japanese).
6. Fukuoka, S., H. Miyazaki, H. Ohgushi, and D. Kamura : Flow and bed topography in a meandering compound channel with phase difference between the alignment of the main channel and levee, Annual Journal of Hydraulic Engineering, JSCE, Vol.40, pp.941-946, 1996, (in Japanese).
7. Muto, Y., K. Shiono, H. Imamoto, and T. Ishigaki : 3-Dimensional structure for overbank flow in meandering channel, Annual Journal of Hydraulic Engineering, JSCE, Vol.40, pp.711-716, 1996, (in Japanese).
8. Fukuoka, S., H. Ogushi, D. Kamura, and S. Hirao : Hydraulic characteristics of the flood flow in a compound meandering channel Journal of Hydraulic, Coastal and Environmental Engineering, JSCE, No.579/II-41, pp.83-92, 1997, (in Japanese).
9. Fukuoka, S., A. Watanabe, D. Kamura, and S. Okada : Study of rate of bed load and bed topography in a meandering compound channel, Annual Journal of Hydraulic Engineering, JSCE, Vol.41, pp.883-888, 1997, (in Japanese).
10. Fukuoka, S., H. Takahashi and D. Kamura : Compound meandering flow and simple meandering flow in compound meandering rivers-Analysis by the use of aerophotograph flood flow velocity vector, Annual Journal of Hydraulic Engineering, JSCE, Vol.41, pp.971-976, 1997, (in Japanese).
11. Jin, H.S., S. Egashira, and B.Y. Liu : Characteristics of meandering compound channel flow evaluated with two-layered, 2-D method, Annual Journal of Hydraulic Engineering, JSCE, Vol.40, pp.717-724, 1996.
12. Jin. H.S., S. Egashira, B.Y. Liu and M. Sumino : Evaluation of velocity near bed in meandering compound open channel flow, Annual Meeting of the Japan Society of Civil Engineers, Vol.2, pp.618-619, 1997.
13. Jin. H.S., S. Egashira, B.Y. Liu and K. Kitayama : Simulation on bed deformation in meandering compound open channel flow, Annul meeting of the Japan Society of Civil Engineers, Vol.2, pp.505-503, 1997.
14. Watanabe, A. and S. Fukuoka : Analysis of 3-dimensional flow in compound meandering channels, Annual Meeting of the Japan Society of Civil Engineers, pp.334-335, 1996, (in Japanese).
15. Fukuoka, S. and A. Watanabe : Three dimensional analysis on flows in meandering compound channels, Journal of Hydraulic, Coastal and Environmental Engineering, No.586/II-42, pp.39-50, 1998, (in Japanese).
16. Fukuoka, S., A. Watanabe, Y. Kayaba and H. Soda : Flow and bed profiles in curved channels with discontinuously installed vanes, Journal of Hydraulic, Coastal and environmental Engineering, JSCE, No.479/II-25, pp.61-70, 1993, (in Japanese).
17. Fukuoka, S. and M. Yamasaka : Alternating bars in a straight channel, Proc. of the 27th Japanese Conference on Hydraulics, pp.703-708, 1983, (in Japanese).

(Received October 12, 1998 ; revised September 14, 1999)